Abstract

Object

Myelomeningocele (MMC) is the most severe form of spina bifida causing severe neurological deficits. Injury to the placode has been attributed to in utero aggression. In this study, glial and neuronal cell changes in both number and topography in mice with MMC were investigated during gestation.

Methods

The curly tail/looptail mice model of MMC was used, and fetuses were harvested using caesarean surgery at Days 14.5, 16.5, and 18.5 (full gestation at 19 days). Immunohistochemical analyses of the MMC placodes and the normal spinal cords from the control group were performed using anti–glial fibrillary acidic protein (astrocytes) and mouse anti–neuronal nuclear (neurons) antibodies. Light microscopy was used along with computer-assisted morphometric evaluation.

Progressive increases in astrocytes in the spinal cord of all mouse fetuses were found between Days 14.5 and 18.5 of gestation. This increase was significantly higher in the placodes of mice with MMC than in those of normal mice, particularly in the posterior region. Neuronal labeling at Day 14.5 of gestation was similar between mice with MMC and control mice. At Day 16.5 of gestation there was a deterioration of neural tissue in MMC fetuses, mainly in the posterior region, progressing until the end of gestation with a marked loss of neurons in the entire MMC placode.

Conclusions

This study delineated the quantitative changes in astrocytes and neurons associated with MMC development during the late stages of gestation. The detailed topographic analysis of the MMC defines the timing of the intrauterine insult and how the placode lesions progress. This study supports the current concept of placode protection through in utero surgery for fetuses with MMC.

KEYWORDS:myelomeningocele; astrocyte; neuronal cell; immunohistochemistry; fetal surgery; pediatric neurosurgery.

Introduction

Spina bifida aperta, or MMC, is a primary neurulation defect that is associated with a significant morbidity and mortality rate in the affected children.[6,12,15,34] Myelomeningocele occurs in nearly 1 in every 2000 live births,[29,44] even in countries where maternal folic acid supplementation and an early in utero diagnosis of MMC is available.[6,34,35] Myelomeningocele leads to lifelong and devastating physical disability; MMC newborns present with different degrees of lower extremity paralysis, sexual organ and sphincter dysfunction, tethering of the spinal cord, skeletal abnormalities, brainstem dysfunction, and hydrocephalus, and may develop disorders that require the insertion of ventriculoperitoneal shunts.[3,34,38,43] The mortality rate in children with MMC ranges from 14 to 35% until they reach the age of 5 years.[16,34,44,45]

The precise cause of spina bifida is unknown, and is probably of a multifactorial nature.[12,33] Data from the experimental induction of MMC in animal models have raised questions about the previously dominant concept of an intrinsic embryonic error causing MMC neurological deficits,[14,22,27,31–33] and these data have supported the hypothesis of a distressed intrauterine environment as a cause of MMC, either by trauma or chemical injury of the placode.[13,17] The histological evaluation of the human MMC placode has shown different degrees of injury as great as a total loss of neural tissue.[26] The findings that ventral remnants of the MMC spinal cord often show normal development together with injury of the dorsal spinal cord appears to be a recent phenomenon, and supports a mechanical factor as a cause of the spinal cord with MMC.[26] Additionally, recent studies using electromyograms of newborns with MMC and clinical lower limb deficits have revealed early neonatal denervation potentials that suggest lower motor neuron damage occurred

during the last weeks of intrauterine development.[41] Fetal surgery was recently initiated as an experimental treatment of MMC with the goal of protecting the neural placode by covering the exposed spinal segments of the MMC.[8,9,44,46,47] This procedure has achieved excellent results in relation to reversing the associated hindbrain herniation, as well as reducing (from 91 to 59%) the need for insertion of a shunt.[2,8,9,36,48,49] The benefits of the surgical treatment of MMC have not been as promising for lower limb deficits and urodynamic function; this procedure is currently being evaluated in a randomized trial.[7,10,23–25,34,43,45,51]

The etiology and natural history of placode deterioration in MMC remains unclear and this issue has important therapeutic implications for the treatment of MMC. To contribute to a better understanding of the MMC placode cytopathology and in utero changes, we have performed an immunohistochemical characterization of the spinal cord cells (neurons and astrocytes) during the gestation of mutant mice with MMC. Two mutant mouse lineages (curly tail/looptail, ct/lp) were utilized because they are associated with severe spina bifida. The ct/lp model of MMC has been used before[42] and was chosen to characterize the topographical changes that occur in the placode during gestation. These alterations were defined through a morphometric analysis of immunostained glial and neuronal cells.

Materials and Methods

Go to section

Animal Model and Experimental Design

We used mice that harboured both ct and lp mutations because they often produce severe spina bifida.[42] The mouse mutant expressing the ct mutation was purchased from the Jackson Laboratory and the lp mutation mouse was offered to us by Dr. Andrew Copp (Neural Development Unit, Institute of Child Health, University College London). The mice were housed in a controlled temperature room that was maintained with a 12-hour light/dark cycle. Water and food were available ad libitum. Mice were treated according to the "Guide for the Care and Use of Laboratory Animals" published by the US National Institutes of Health (NIH Publication No. 85-23, revised 1996), and the European Union law on animal protection (Directive 86/609/EC).

Mice with MMC were obtained by mating doubly heterozygous ct/lp male mice with homozygous ct female mice. Female mice were monitored daily for the presence of vaginal plugs and the day a plug appeared was defined as gestational Day 0.5.[37,42] Fetuses were harvested by caesarean surgery at Days 14.5, 16.5, and 18.5 of gestation (full gestation at 19 days). Newborns of the same gestational ages with normal hindlimb function and showing no MMC were used as controls.

Experimental Protocol

Newborn pups with the MMC defect were obtained by elective caesarean at embryonic Days 14.5, 16.5 and 18.5. Three experimental groups composed of six mice with MMC in each group were formed, and they were compared with three control groups that had the same number of specimens with the same gestational age. For clinical assessment, live-born pups were weighed and measured; they were also examined for neurological deficits by assessing postural reaction and pain perception by lightly pricking the skin of the hind limb with a hemostat.[4]

Pregnant mice were killed by a combined lethal injection of keta-mine and xylazine hydrochloride (Bayer) immediately before caesarean surgery was performed for fetal harvesting. Embryos were fixed in a buffered solution of 4% paraformaldehyde with 14% picric acid for 1 hour. The specimens were cut through the axial plane of the spine to include the MMC placode. These samples were further fixed for 24 hours in the same fixative before tissue processing and paraffin embedment. Three-micrometer sections were obtained and mounted on poly-L-lysine-coated glass slides. After dewaxing in xylene and re-hydration using graded ethanol, the samples were incubated in 3% hydrogen peroxide in methanol to quench endogenous peroxidase. Antigen retrieval was achieved by boiling the sample in a 10-mM citrate buffer (pH 6.0) and then cooling it down to room temperature. Samples were rinsed rapidly in water, washed in PBS, and incubated in Ultra V Block (UltraVision Detection System, Lab Vision) for 20 minutes at room temperature to block nonspecific staining. Incubation with primary antibodies was done with anti-GFAP (1:1250) or anti-NeuN (1:100) for 1 hour at room temperature.

Immunohistochemistry analysis using polyclonal rabbit anti-GFAP antibody Z 0334 (Dako Cytomation) and mouse monoclonal anti-NeuN antibody MAB377 (Chemicon International) was performed according to the same protocol. Incubation with the secondary antibody, biotinylated goat anti-polyvalent serum (UltraVision Detection System, Lab

Vision), was conducted at room temperature for 30 minutes after first rinsing it with PBS. The slides were then washed in PBS, and incubated in streptavidin peroxidase (UltraVision Detection System, Lab Vision) at room temperature for 30 minutes. After several more washings in PBS, the reaction product was detected as a brown substrate using diaminobenzidine tetrahydrochloride (Sigma). The tissue sections were counterstained with hematoxylin. Negative control reactions consisted of omission of the primary antibody. Positive control reactions for both antibodies were performed using tissue sections of the mouse brain. Tissue sections from all animals for each antibody were tested on the same day for antibody staining using the same reagents in order to minimize interassay variability.

Morphometric Analysis

Computer-assisted morphometric evaluation was performed using the image analysis toolkit Leica Qwin. On each slide, immunoreactive spinal cord cells were identified and traced by the software using an objective lens at a magnification of 40 in a predefined square area of 13,100 μm^2. In each of the areas, the number of immunoreactive cells was counted and the proportion of cells per square micrometers was calculated. High magnification micrographs of each spinal cord section were obtained in six different areas as follows: three from the ventral area (including the anterior gray and white columns and the pericentral canal area) and three from the dorsal area of the spinal cord. In the MMC groups, the studied areas were homologous with three ventral and three dorsal areas. The first ventral area was the basal plate (medial), the second the alar plate (lateral), and the third an intermediate area around the sulcus limitans.

Statistical Analysis

Statistical analyses were performed using a two-tailed, unpaired t-test. A probability value less than 0.05 was considered statistically significant. All quantitative data are presented as means ± standard error of the means.

Results

Go to section

The MMC defect was present in one third of the offspring that resulted from mating a double heterozygous ct/lp male mouse with a homozygous ct female mouse. Live-born mice with MMC showed hypotonic hind limbs with spontaneous and extensive movement of the hip and knee joints, but only a slight movement of the ankle joints, compared with the normal animals. No forelimb–hindlimb coordination was observed in the mice with MMC; occasionally, these mice performed plantar steps that demonstrated the ability to support their body weight. Clinical assessment of newborn mice with MMC revealed similar neurological defects in all of these mice. All of the mouse fetuses (both MMC and normal mice) obtained at Days 14.5 and 16.5 of gestation presented with hypotonic limbs with limited movement, thus not allowing the identification of clinical neurological differences between MMC and normal pups. Fetuses of the ct/lp mutant mice presented with lower average weight when they had MMC than in fetuses with no spinal cord defect, but there were no statistically significant weight differences between these groups. The length of the MMC increased during fetal development of the affected mice (Table 1).

TABLE 1 *Summary of the weight and length of ct/lp fetuses with and without MMC*[*]

Histology of MMC

Light microscopy of the MMC fetuses revealed severe structural abnormalities in the spinal cord characterized by the dorsal region of the neural tube lying laterally with regard to the ventral horn, and the dorsal white matter having moved into a ventrolateral position (Fig. 1). The MMC placode of fetuses at Day 14.5 or 16.5 presented with a protruding shape to the skin layer (Figs. 2E and F and 3E and F). This feature became less evident in later gestational stages. The cell lining was preserved on the posterior region of the placode (Figs. 2I and 3I). In normal fetuses, the dorsal, ventral, and lateral columns of the spinal cord were well developed (Figs. 2A–C and 3A–C). The central region of the spinal cord was oval shaped in Day 14.5 fetuses and was covered by numerous dividing neuroepithelial cells that underwent reduction as gestation progressed (Figs. 2C and 3C). In addition, a thin

outer layer of white matter developed during gestation, in particular in the ventral region of the spinal cord (Figs. 2A–C and 3A–C).

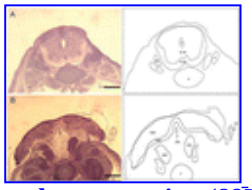

View larger version (89K)

Fig. 1. Photomicrographs of tissue sections from ct/lp mice with a normal spinal cord (A) and a myelomeningocele placode (B) at Day 14.5 of gestation. To the right of each photomicrograph is a drawing showing the topography of major anatomical elements of the spinal cord of the mouse fetus in each condition. H & E, bar = 300 μm. ASA = anterior spinal artery; CC = central canal; DRG = dorsal root ganglia; LM = leptomeninges; PGM = placode gray matter; PWM = placode white matter; SC-GM = spinal cord gray matter; SC-WM = spinal cord white matter; V = vertebra.

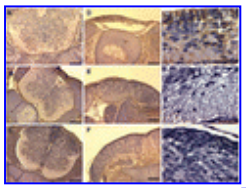

View larger version (180K)

Fig. 2. Photomicrographs of immunostained paraffin-embedded tissue sections showing differences in astrocyte density in the developing spinal cord between samples from control mice without MMC (A–C) and samples of mutant mice (ct/lp) with MMC (D–I). All photomicrographs show cross-sections with the posterior spinal cord positioned at the top of the figure. The astrocytes were labeled by immunoperoxidase (brown staining) using an antibody specific for GFAP; background tissue staining was done with hematoxylin. Three different areas of the placode in control animals are depicted and compared with similar regions of the placode in mice with MMC. At the end of gestation (Day 18.5), in the posterior end of the placode, astrocyte density is lower in the control sample (A) than in the MMC sample (D); panel G shows panel D at a higher magnification. At Day 16.5 of gestation, there are fewer GFAP-positive cells both in the control sample (B) and in the characteristic winglike arrangement of the protruding MMC placode (E); panel H shows panel E at a higher magnification, illustrating the anterior MMC region. At Day 14.5 of gestation, the normal spinal (C) and the MMC placode (F) are samples almost devoid of GFAP labeling; panel I shows panel F at a higher magnification, demonstrating an outer area of cells from the posterior region of MMC. Bar = 150 μm (A–F), 40 μm (G–I).

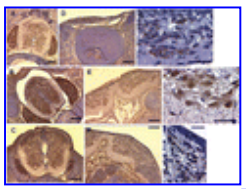

View larger version (167K)

Fig. 3. Photomicrographs of immunostained paraffin-embedded tissue sections showing differences in the distribution of neuronal cells (NeuN-staining) of the developing spinal cord between samples from control mice (without MMC, A–C) and samples from mutant mice (ct/lp) with MMC (D–I). All photomicrographs show cross-sections with the posterior spinal cord positioned at the top of the figure. The neuronal cells were labeled by immunoperoxidase (brown staining) using an antibody specific for NeuN antigen; background tissue staining was done with hematoxylin. At the end of gestation (Day 18.5), the normal spine cord (A) and MMC placode (D) show clear staining of the gray matter. The MMC has a flat appearance with an apparently preserved lining of small stained cells (G). At Day 16.5 of gestation, there are more positive cells both in the control sample (B) and in the MMC protruding placode (E); panel H is a higher magnification of panel E, illustrating the anterior MMC region with large motor neuronal cells. At Day 14.5 of gestation, the normal spinal cord (C) and MMC placode (F) show dense NeuN labeling; panel I is a higher magnification of panel F, showing stained cells in the dorsal MMC region. Bar = 150 μm (A–F), 40 μm (G–I).

Immunohistochemical Analysis of Astrocytes in MMC

An anti-GFAP antibody was used to label astrocytes in situ in the spinal cord of the mice. This immunohistochemical method was applied to serial transverse sections made through the length of the placode. Qualitative observation of the tissue slides indicated that astrocyte labeling was higher in the MMC spinal cord than in that of normal mice. The staining was particularly evident at the posterior region of the MMC placode (Fig. 2D and G). Astrocyte staining also appeared to increase during gestation (Fig. 2). In order to clarify these observations, morphometric analysis of the astrocyte labeling was performed in 36 areas (in six specimens of each group of mice) to obtain data on the number of labeled cells per square micrometers. A statistical comparison of these data revealed a progressive increase in astrocytes in the spinal cords of mouse fetuses during the last stages of gestation, between Days 14.5 and 18.5 (Fig. 4). This enhancement in astrocytes during gestation was significantly higher in the spinal cords of MMC mice than in that of normal mice (Fig. 4). Astrocytosis was also particularly evident in the posterior region of the MMC placode, and was significantly higher in this area than in the anterior region (Fig. 4 *lower*). The comparison between the control mice and MMC mice showed a significant increase in astrocyte density at Days 16.5 ($p < 0.01$) and 18.5 ($p < 0.001$) of gestation for the posterior region of the placode, and at the end of gestation (Day 18.5) for the anterior region ($p < 0.001$).

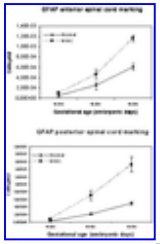

View larger version (46K)

Fig. 4. Graphs of the morphometric analysis of GFAP (astrocyte) staining of the anterior *(upper)* and posterior *(lower)* regions of the spinal cord during mouse gestation. Significant differences in astrocyte density were found between fetuses of the mutant ct/lp mice with MMC and of control mice (without MMC). Increases in the density of GFAP-stained spinal cord astrocytes occurred at the end (Days 14.5–18.5) of the mouse fetal period. The comparison between mice with MMC and control mice showed a significant enhancement in astrocyte density at Days 16.5 ($p < 0.01$) and 18.5 ($p < 0.001$) of gestation for the posterior region of the placode, and at the end of gestation (Day 18.5) for the anterior region ($p < 0.001$).

Immunohistochemical Analysis of Neuronal Cells in MMC

An anti-NeuN antibody was used to label neuronal cells in the spinal cord of the mice. At Day 14.5 of gestation, the staining of neuronal cells in the MMC placode appeared to be similar to that of the spinal cord of normal mice (Fig. 3). The staining was abundant and was particularity intense on gray columns. The dorsal horns of the normal placode were also well labeled (Fig. 3), whereas in the MMC placode, neuronal labeling was slightly more extensive on its posterior than on its anterior region. Morphometric analysis of neuronal cell labeling was performed in the same manner as it was for astrocyte quantification (see previous section). A statistical comparison of data revealed that MMC placodes showed a significantly lower number of neuronal cells than the normal placode, and that the cell density of neurons in the MMC placode decreased during the final stages of spinal cord development, between Days 14.5 and 18.5 of gestation (Fig. 5). In comparison with control mice with a normal spinal cord, mice with the MMC placode show a significant decrease in neuronal cell density at Day 16.5 ($p < 0.05$) and Day 18.5 ($p < 0.01$) of gestation for the posterior region of the placode, and at the end of gestation (Day 18.5) for the anterior region ($p < 0.05$).

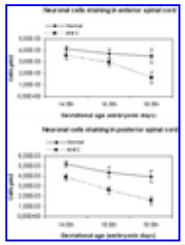

View larger version (48K)

Fig. 5. Graphs of the morphometric analysis of NeuN staining of the anterior *(upper)* and posterior *(lower)* regions of the spinal cord during mouse gestation. Significant differences in neuronal cell density were found between fetuses of mutant mice (ct/lp) with MMC and samples from fetuses of control mice (without MMC). A decrease in the density of NeuN-stained neuronal cells of the spinal cord occurred at the end (Days 14.5–18.5) of the mouse fetal period. In comparison with control mice, mice with MMC show a significant decrease in neuronal cell density at Day 16.5 ($p < 0.05$) and 18.5 ($p < 0.01$) of gestation for the posterior region of the placode, and at end of gestation (Day 18.5) for the anterior region ($p < 0.05$).

Discussion

Go to section

The severity of the handicap in infants with spina bifida depends on the segmental level of the lesion; some infants have no disability, others have impaired urogenital and/or motor function.[23,34,44,45] Neuronal maturation and placode preservation are the definitive factors in the functional prognosis of MMC.[5,32] Previous investigators using mutant mouse models have demonstrated an unaltered early gestational neurogenesis.[28,30,39] According to the two–hit hypothesis, the MMC lesions have been ascribed to an initial error in embryogenesis followed by a secondary injury factor.[12,31,32] Proposed secondary injuries of MMC are putative trauma or chemical injury.[26,32,43] To better understand MMC, it is pertinent to investigate MMC placode structural changes during the gestational period when placode insult is likely to occur. We have addressed this issue by performing a morphometric analysis in different areas of the MMC mutant mice placode that were labeled by immunohistochemistry.

This investigation has defined the cellular dynamics of astrocytes and neurons during the late stages of the development of the spinal cord in utero in both normal mice and in MMC mutant mice. We documented a clear enhancement in astrocyte labeling in the placode, mainly in the dorsal area of the placode and during the late stages of gestation. This phenomenon is evident at Day 16.5 of gestation for the posterior region and at full gestation for all of the placode. The finding of neuronal cell labeling on dysraphic neural tissue at Day 14.5 of gestation indicated a normal early differentiation of neurons, followed by rapid and progressive deterioration of neural tissue mainly in the posterior region of the placode that was observed at Day 16.5 of gestation. This process continued and at full gestation there was a marked loss of neurons in all MMC placodes of mutant mice.

These results strengthen the general assumption that the MMC placode is an open dysraphic tube with a primary neurulation insult that occurs after a normal early neuro-genesis.[12,20,29,39] It is well established that the MMC placode experiences aggression that induces astrocytosis.[19,26] Recent clinical and electromyographic studies in humans have shown that neonatal loss of motor function is clearly initiated at a prenatal stage.[41] Amniotic fluid levels of brain-specific proteins in mutant mice with MMC showed a significant increase in astrocyte antigen on Day 16.5 of gestation.[37] Our results add detailed information using microscopy on how astrocytosis occurs and how it progresses in the MMC placode of the ct/lp mutant mouse, namely that astrocytosis is a continuing process during the latter third part of mouse gestation, and that it starts in the dorsal region and spreads to all of the placode.

Keller-Peck and Mullen[29] have described neuronal degeneration of the MMC at Day 17 of gestation in the ct mouse model of MMC. We observed similar changes and augmented them with evaluation of anterior and posterior regions of the MMC. Our findings revealed that this degeneration starts earlier, and is more intense in the dorsal region of the MMC placode, indicating that this area is probably experiencing a more severe injury. It is likely that this injury induces astrocytic cell proliferation and loss of neuronal cells.

The documented focal nature of the initial lesions observed in the MMC placode in this study does not favor consideration of the MMC as the result solely of an intrinsic embryonic error. This interpretation is further supported by our finding that the loss of neurons and the astrocytosis do not predominate in the alar versus basal plate or marginal versus mantle layer, but rather are predominant on the posterior region of the placode in comparison with the anterior region. A multitude of factors may be involved in this injury. In the ct mouse model of MMC, it is understood that until Day 11 of gestation the spinal cord and the MMC pla-code are not exposed to the amniotic fluid,[29] which may allow an early normal

neurogenesis. The latter neuronal degeneration of MMC perhaps may be explained by the abnormal absence of cerebrospinal fluid that normally covers and protects the placode. It is also plausible that the embryonic insult makes the placode more fragile to intrauterine challenges during development, namely by becoming more susceptible to ischemic phenomena. Another putative factor for injury could be the likelihood that a larger fetus in the final stages of gestation experiences intrauterine trauma. Support for this injury factor is found in the structural abnormalities of human fetuses undergoing trauma because the neural tissue is found to be lost almost exclusively in the dorsal portion of the MMC.[26] Our results indicate a more posterior insult. Our findings are difficult to explain by mechanical factors alone because in all our specimens of murine MMC placodes there was preservation of the cellular lining of the dorsal surface of the placode. It has been reported that human amniotic fluid after 34 weeks of gestation is toxic for experimental cultures of rat spinal cord cells.[17] Although this injury factor cannot be discarded in our mutant mouse model of MMC, the placode maturation became altered earlier in gestation, just after Day 14.5.

Recent data from intrauterine surgical correction of human MMC showed a clear benefit in the treatment of hind-brain herniation, reducing to approximately half the number of cases that needed the insertion of a ventriculoperitoneal shunt.[8,9,46,48] The neurological benefit for the lower limb function from this surgical treatment was, however, limited to two-level spinal improvement.[8,23,25,34,40,45,47–50] The pathophysiological finding of an apparent initially normal maturation that is interrupted later suggests that correction of MMC during gestation should be a good therapeutic approach. Certainly, the development of neuroimaging for prenatal evaluation, the risks associated with an intrauterine intervention, the technical advancements of in utero surgery, and the optimal timing for performing the procedure are all other important determinants contributing to the success of the surgery.[1,7,11,18,21,49,52]

Conclusions

Immunohistochemical analysis of the MMC placode during the gestation of ct/lp mice indicates that the initial neuronal differentiation of the MMC placode is similar to that of the normal spinal cord. The MMC degeneration in this mutant mouse model involves progressive loss of neuronal cells and increases in astrocytes; these changes are of a focal nature and are more evident on the posterior region of the placode. These data support the potential benefit of in utero surgical treatment of infants with MMC, by providing protection of the placode tissue from chemical and mechanical injury during the last stages of fetal development.

Acknowledgments

We would like to thank Professor A. J. Copp (Neural Development Unit, Institute of Child Health, University College London, United Kingdom) for his kind offer of breeding pairs for the mutant mouse model. We also thank the excellent technical support of Dr. Madalena Costa and are grateful to Mrs. Alexandrina Ribeiro for laboratory help.

References

1. Aaronson OS, Hernanz-Schulman M, Bruner JP, Reed GW, Tulipan NB: Myelomeningocele: prenatal evaluation—comparison between transabdominal US and MR imaging. Radiology 227:839–843, 2003 [CrossRef] [Medline]
2. Adzick NS, Sutton LN, Crombleholme TM, Flake AW: Successful fetal surgery for spina bifida. Lancet 352:1675–1676, 1998 [CrossRef] [Medline]
3. Babcook CJ, Goldstein RB, Barth RA, Damato NM, Callen PW, Filly RA: Prevalence of ventriculomegaly in association with myelomeningocele: correlation with gestational age and severity of posterior fossa deformity. Radiology 190:703–707, 1994 [Medline]
4. Basso DM, Beattie MS, Bresnahan JC: A sensitive and reliable locomotor rating scale for open field testing in rats. J Neurotrauma 12:1–21, 1995 [CrossRef] [Medline]

5. Beuls EA, Vanormelingen L, van Aalst J, Vandersteen M, Adriaensen P, Cornips EM, et al.: In vitro high-field magnetic resonance imaging-documented anatomy of a fetal myelomeningocele at 20 weeks' gestation. A contribution to the rationale of intrauterine surgical repair of spina bifida. J Neurosurg 98:2 Suppl210–214, 2003 [Abstract] [Medline]
6. Brand MC: Examining the newborn with an open spinal dysraphism. Adv Neonatal Care 6:181–196, 2006 [CrossRef] [Medline]
7. Bruner JP, Tulipan N, Dabrowiak ME, Luker KS, Walters K, Burns P, et al.: Upper level of the spina bifida defect: how good are we?. Ultrasound Obstet Gynecol 24:612–617, 2004 [CrossRef] [Medline]
8. Bruner JP, Tulipan N, Paschall RL, Boehm FH, Walsh WF, Silva SR, et al.: Fetal surgery for myelomeningocele and the incidence of shunt-dependent hydrocephalus. JAMA 282:1819–1825, 1999 [CrossRef] [Medline]
9. Bruner JP, Tulipan N, Reed G, Davis GH, Bennett K, Luker KS, et al.: Intrauterine repair of spina bifida: preoperative predictors of shunt-dependent hydrocephalus. Am J Obstet Gynecol 190:1305–1312, 2004 [CrossRef] [Medline]
10. Cochrane DD, Irwin B, Chambers K: Clinical outcomes that fetal surgery for myelomeningocele needs to achieve. Eur J Pediatr Surg 11:1 SupplS18–S20, 2001 [CrossRef] [Medline]
11. Coleman BG, Adzick NS, Crombleholme TM, Johnson MP, Howell L, Horii SC, et al.: Fetal therapy: state of the art. J Ultrasound Med 21:1257–1288, 2002 [Medline]
12. Copp AJ, Greene ND, Murdoch JN: The genetic basis of mammalian neurulation. Nat Rev Genet 4:784–793, 2003 [CrossRef] [Medline]
13. Correia-Pinto J, Reis JL, Hutchins GM, Baptista MJ, Estevao-Costa J, Flake AW, et al.: In utero meconium exposure increases spinal cord necrosis in a rat model of myelomeningocele. J Pediatr Surg 37:488–492, 2002 [CrossRef] [Medline]
14. Danzer E, Schwarz U, Wehrli S, Radu A, Adzick NS, Flake AW: Retinoic acid induced myelomeningocele in fetal rats: characterization by histopathological analysis and magnetic resonance imaging. Exp Neurol 194:467–475, 2005 [CrossRef] [Medline]
15. Dias MS, Partington M: Embryology of myelomeningocele and anencephaly. Neurosurg Focus 16:2E1, 2004 [Abstract] [Medline]
16. Dillon CM, Davis BE, Duguay S, Seidel KD, Shurtleff DB: Longevity of patients born with myelomeningocele. Eur J Pediatr Surg 10:1 Suppl33–34, 2000 [CrossRef] [Medline]
17. Drewek MJ, Bruner JP, Whetsell WO, Tulipan N: Quantitative analysis of the toxicity of human amniotic fluid to cultured rat spinal cord. Pediatr Neurosurg 27:190–193, 1997 [CrossRef] [Medline]
18. Farmer DL, von Koch CS, Peacock WJ, Danielpour M, Gupta N, Lee H, et al.: In utero repair of myelomeningocele: experimental pathophysiology, initial clinical experience, and outcomes. Arch Surg 138:872–878, 2003 [CrossRef] [Medline]
19. George TM, Cummings TJ: The immunohistochemical profile of the myelomeningocele placode: is the placode normal?. Pediatr Neurosurg 39:234–239, 2003 [CrossRef] [Medline]
20. George TM, Fuh E: Review of animal models of surgically induced spinal neural tube defects: implications for fetal surgery. Pediatr Neurosurg 39:81–90, 2003 [CrossRef] [Medline]
21. Hamdan AH, Walsh W, Heddings A, Bruner JP, Tulipan N: Gestational age at intrauterine myelomeningocele repair does not influence the risk of prematurity. Fetal Diagn Ther 17:66–68, 2002 [CrossRef] [Medline]
22. Heffez DS, Aryanpur J, Hutchins GM, Freeman JM: The paralysis associated with myelomeningocele: clinical and experimental data implicating a preventable spinal cord injury. Neurosurgery 26:987–992, 1990 [CrossRef] [Medline]
23. Hirose S, Meuli-Simmen C, Meuli M: Fetal surgery for myelomeningocele: panacea or peril?. World J Surg 27:87–94, 2003 [CrossRef] [Medline]
24. Holmes NM, Nguyen HT, Harrison MR, Farmer DL, Baskin LS: Fetal intervention for myelomeningocele: effect on postnatal bladder function. J Urol 166:2383–2386, 2001 [CrossRef] [Medline]
25. Holzbeierlein J, Pope JI IV, Adams MC, Bruner J, Tulipan N, Brock JW III: The urodynamic profile of myelodysplasia in childhood with spinal closure during gestation. J Urol 164:1336–1339, 2000 [CrossRef] [Medline]

26. Hutchins GM, Meuli M, Meuli-Simmen C, Jordan MA, Heffez DS, Blakemore KJ: Acquired spinal cord injury in human fetuses with myelomeningocele. Pediatr Pathol Lab Med 16:701–712, 1996 [CrossRef] [Medline]

27. Julia V, Sancho MA, Albert A, Conill J, Martinez A, Grande C, et al.: Prenatal covering of the spinal cord decreases neurologic sequelae in a myelomeningocele model. J Pediatr Surg 41:1125–1129, 2006 [CrossRef] [Medline]

28. Keller-Peck CR, Mullen RJ: Altered cell proliferation in the spinal cord of mouse neural tube mutants curly tail and Pax3 splotch-delayed. Brain Res Dev Brain Res 102:177–188, 1997 [CrossRef] [Medline]

29. Keller-Peck CR, Mullen RJ: Patterns of neuronal differentiation in neural tube mutant mice: curly tail and Pax3 splotch-delayed. J Comp Neurol 368:516–526, 1996 [CrossRef] [Medline]

30. McLone DG, Dias MS, Goossens W, Knepper PA: Pathological changes in exposed neural tissue of fetal delayed splotch (Spd) mice. Childs Nerv Syst 13:1–7, 1997 [CrossRef] [Medline]

31. Meuli M, Meuli-Simmen C, Hutchins GM, Seller MJ, Harrison MR, Adzick NS: The spinal cord lesion in human fetuses with myelomeningocele: implications for fetal surgery. J Pediatr Surg 32:448–452, 1997 [CrossRef] [Medline]

32. Meuli M, Meuli-Simmen C, Hutchins GM, Yingling CD, Hoff-man KM, Harrison MR, et al.: In utero surgery rescues neurological function at birth in sheep with spina bifida. Nat Med 1:342–347, 1995 [CrossRef] [Medline]

33. Meuli-Simmen C, Meuli M, Adzick NS, Harrison MR: Latissimus dorsi flap procedures to cover myelomeningocele in utero: a feasibility study in human fetuses. J Pediatr Surg 32:1154–1156, 1997 [CrossRef] [Medline]

34. Mitchell LE, Adzick NS, Melchionne J, Pasquariello PS, Sutton LN, Whitehead AS: Spina bifida. Lancet 364:1885–1895, 2004 [CrossRef] [Medline]

35. Padmanabhan R: Etiology, pathogenesis and prevention of neural tube defects. Congenit Anom (Kyoto) 46:55–67, 2006 [CrossRef] [Medline]

36. Paek BW, Farmer DL, Wilkinson CC, Albanese CT, Peacock W, Harrison MR, et al.: Hindbrain herniation develops in surgically created myelomeningocele but is absent after repair in fetal lambs. Am J Obstet Gynecol 183:1119–1123, 2000 [CrossRef] [Medline]

37. Petzold A, Stiefel D, Copp AJ: Amniotic fluid brain-specific proteins are biomarkers for spinal cord injury in experimental myelomeningocele. J Neurochem 95:594–598, 2005 [CrossRef] [Medline]

38. Rintoul NE, Sutton LN, Hubbard AM, Cohen B, Melchionni J, Pasquariello PS, et al.: A new look at myelomeningoceles: functional level, vertebral level, shunting, and the implications for fetal intervention. Pediatrics 109:409–413, 2002 [CrossRef] [Medline]

39. Selcuki M, Vatansever S, Inan S, Sanci M, Sayhan S, Bagdatoglu C: Neural tissue continues its maturation at the site of neural tube closure defects: implications for prenatal intervention in human samples. Childs Nerv Syst 20:313–320, 2004 [CrossRef] [Medline]

40. Simpson JL: Fetal surgery for myelomeningocele: promise, progress, and problems. JAMA 282:1873–1874, 1999 [CrossRef] [Medline]

41. Sival DA, van Weerden TW, Vles JS, Timmer A, den Dunnen WF, Staal-Schreinemachers AL, et al.: Neonatal loss of motor function in human spina bifida aperta. Pediatrics 114:427–434, 2004 [CrossRef] [Medline]

42. Stiefel D, Shibata T, Meuli M, Duffy PG, Copp AJ: Tethering of the spinal cord in mouse fetuses and neonates with spina bifida. J Neurosurg 99:2 Suppl206–213, 2003 [Abstract] [Medline]

43. Sutton LN, Adzick NS, Bilaniuk LT, Johnson MP, Crombleholme TM, Flake AW: Improvement in hindbrain herniation demonstrated by serial fetal magnetic resonance imaging following fetal surgery for myelomeningocele. JAMA 282:1826–1831, 1999 [CrossRef] [Medline]

44. Sutton LN, Adzick NS, Johnson MP: Fetal surgery for myelomeningocele. Childs Nerv Syst 19:587–591, 2003 [CrossRef] [Medline]

45. Sutton LN, Sun P, Adzick NS: Fetal neurosurgery. Neurosurgery 48:124–144, 2001 [CrossRef] [Medline]

46. Tulipan N: Intrauterine myelomeningocele repair. Clin Perinatol 30:521–530, 2003 [CrossRef] [Medline]

47. Tulipan N, Bruner JP, Hernanz-Schulman M, Lowe LH, Walsh WF, Nickolaus D, et al.: Effect of intrauterine myelomeningocele repair on central nervous system structure and function. Pediatr Neurosurg 31:183–188, 1999 [CrossRef] [Medline]

48. Tulipan N, Hernanz-Schulman M, Lowe LH, Bruner JP: Intra-uterine myelomeningocele repair reverses preexisting hindbrain herniation. Pediatr Neurosurg 31:137–142, 1999 [CrossRef] [Medline]

49. Tulipan N, Sutton LN, Bruner JP, Cohen BM, Johnson M, Adzick NS: The effect of intrauterine myelomeningocele repair on the incidence of shunt-dependent hydrocephalus. Pediatr Neurosurg 38:27–33, 2003 [CrossRef] [Medline]

50. Wagner W, Schwarz M, Perneczky A: Primary myelomeningocele closure and consequences. Curr Opin Urol 12:465–468, 2002 [CrossRef] [Medline]

51. Walsh DS, Adzick NS: Foetal surgery for spina bifida. Semin Neonatol 8:197–205, 2003 [CrossRef] [Medline]

52. Wilson RD: Prenatal evaluation for fetal surgery. Curr Opin Obstet Gynecol 14:187–193, 2002 [CrossRef] [Medline]

Cited by

Joaquim L. Reis, M.D., Ph.D., Jorge Correia-Pinto, M.D., Ph.D., Mariana P. Monteiro, M.D., Ph.D., Madalena Costa, B.Sc., and Grover M. Hutchins, M.D.. (2008) Vascular and apoptotic changes in the placode of myelomeningocele mice during the final stages of in utero development. *Journal of Neurosurgery: Pediatrics* **2**:2, 150-157
Online publication date: 1-Aug-2008.